

# PD-L1 and tumor-associated macrophages in de novo DLBCL

Ronald McCord,<sup>1,\*</sup> Christopher R. Bolen,<sup>2,\*</sup> Hartmut Koeppen,<sup>3</sup> Edward E. Kadel III,<sup>1</sup> Mikkel Z. Oestergaard,<sup>4</sup> Tina Nielsen,<sup>5</sup> Laurie H. Sehn,<sup>6</sup> and Jeffrey M. Venstrom<sup>1</sup>

<sup>1</sup>Oncology Biomarker Development, <sup>2</sup>Bioinformatics, and <sup>3</sup>Research Pathology, Genentech, South San Francisco, CA; <sup>4</sup>Oncology Biomarker Development and <sup>5</sup>Clinical Development Oncology, Roche, Basel, Switzerland; and <sup>6</sup>Centre for Lymphoid Cancer, British Columbia Cancer Agency, Vancouver, BC, Canada

## Key Points

- 85% to 95% of de novo DLBCL patients express PD-L1, primarily on myeloid cells, and PD-L1 correlated with macrophage and *STAT3* expression.
- PD-L1 did not identify high-risk patients in de novo DLBCL, and may be associated with better prognosis in some patients.

Programmed death-ligand 1 (PD-L1) and its receptor, programmed cell death-1 (PD-1), are important negative regulators of immune cell activation. Therapeutically targeting PD-1/PD-L1 in diffuse large B-cell lymphoma (DLBCL) patients with a single agent has limited activity, meriting a deeper understanding of this complex biology and of available PD-L1 clinical assays. In this study, we leveraged 2 large de novo DLBCL phase 3 trials (GOYA and MAIN) to better understand the biologic and clinical relevance of PD-L1 in de novo DLBCL. PD-L1 was expressed on myeloid cells in 85% to 95% of DLBCL patients (depending on staining procedure), compared with 10% on tumor cells, and correlated with macrophage gene expression. PD-L1 did not identify high-risk patients in de novo DLBCL; it correlated with *STAT3*, macrophage gene expression, and improved outcomes among a subset of patients. These results may help identify immunologically distinct DLBCL subsets relevant for checkpoint blockade. GOYA and MAIN trials were registered at [www.clinicaltrials.gov](http://www.clinicaltrials.gov) as #NCT01287741 and #NCT00486759, respectively.

## Introduction

Programmed death-ligand 1 (PD-L1) and its receptor, programmed cell death-1 (PD-1), are expressed on multiple cell types, including antigen-presenting cells, T cells, and tumor cells (TCs), and negatively regulate immune cell (IC) activation.<sup>1-7</sup> Among de novo diffuse large B-cell lymphoma (DLBCL) patients, high PD-L1 expression and soluble PD-L1 have been correlated with both inferior and superior clinical outcomes, possibly attributable to different patient populations, different PD-L1 reagents, or a more complex PD-L1 biology within this heterogeneous disease.<sup>8-12</sup> In de novo DLBCL patients treated with immunochemotherapy, specific PD-L1 expression by malignant B cells is associated with worse outcome.<sup>8</sup> However, accurate estimation of tumor-specific PD-L1 staining is challenging, with most studies suggesting that tumor-specific PD-L1 expression is rare, possibly limited to a small percentage of the activated B-cell (ABC) subtype of DLBCL, and may depend on the PD-L1 reagent.<sup>8,10,12-14</sup> PD-L1 expression by nonmalignant ICs such as activated monocytes and dendritic cells (DCs) is more common, and this PD-L1 IC staining using SP142 is relevant for anti-PD-L1 clinical responses among lung cancer patients.<sup>8,13,15,16</sup>

In this study, we leveraged samples from 2 large de novo DLBCL phase 3 trials and gene expression data from purified ICs to better understand the biologic and clinical relevance of PD-L1 expression in de novo DLBCL. We report that PD-L1 was primarily expressed on myeloid cells in DLBCL, that expression of PD-L1 correlated with macrophage gene expression, and that PD-L1 was not a negative prognostic biomarker in DLBCL and in fact may have indicated improved prognosis in some patients. In addition, we show that high expression of a macrophage gene signature was associated with improved survival among de novo DLBCL patients treated with immunochemotherapy and that it added prognostic information to the cell-of-origin subsets, in that high expression of the macrophage signature correlated with prolonged progression-free survival (PFS), particularly among the poor-prognosis ABC subset.

Submitted 3 May 2018; accepted 2 January 2019. DOI 10.1182/bloodadvances.2018020602.

\*R.M. and C.R.B. are joint first authors.

The full-text version of this article contains a data supplement.

© 2019 by The American Society of Hematology

## Methods

### Clinical samples

Clinical, genomic, and pretreatment immunohistochemistry (IHC) data were available from patients treated in the GOYA (R-CHOP [rituximab plus cyclophosphamide, doxorubicin, vincristine, and prednisone] vs obinutuzumab plus CHOP)<sup>17</sup> and MAIN (R-CHOP ± bevacizumab)<sup>18</sup> clinical trials (Table 1). The protocols of the original trials were approved by local or national ethics committees according to the laws of each country, and the study was undertaken in accordance with the Declaration of Helsinki. ABC/germinal center B-cell (GCB)/unclassified DLBCL prognostic subtypes were determined by the Nanostring LST assay (GOYA) or by application of the Wright et al<sup>19</sup> algorithm to expression data from a custom Fluidigm gene expression panel containing the 27 genes of the DLBCL subgroup predictor (MAIN). Median follow-up durations were 24 and 29 months for MAIN and GOYA, respectively (~30% of PFS events in both cohorts).

### IHC

IHC assays were performed on pretreatment samples from MAIN (2013) and GOYA (2018) using 2 different PD-L1 IHC reagents (SP142,<sup>20</sup> SP263) and 21 uninvolved lymph node sections as controls. Tissue cores with insufficient or poorly preserved tissue were excluded. The SP142 PD-L1 IHC staining protocol was updated to include tyramide signal amplification (TSA) amplification, which was used for PD-L1 staining in GOYA. Tissue microarray slides consisted of 1-mm cores (2-3 per patient) and were scored based on tissue area occupied by PD-L1<sup>+</sup> cells (ICs and TCs) using the following algorithm: IHC 0, <1%; IHC 1, 1% to 5%; IHC 2, 5% to 10%; and IHC 3, >10%. TCs and ICs were identified based on morphologic and cytologic features, and PD-L1 tumor expression was scored as a percentage of all TCs. PD-L1 expression by malignant cells required the presence of complete, circumferential membranous staining of malignant cells. Interpretation of immunostains was performed by a board-certified hematopathologist.

### Genomics

RNA was isolated and purified from pretreatment formalin-fixed paraffin-embedded biopsies using Qiagen FFPE RNAEasy preparation kits. The purified RNA was used to create complementary DNA libraries that were assayed using TruSeq (Illumina) RNA sequencing (RNAseq) to measure PD-L1, macrophage, and B-cell gene expression among 702 DLBCL patients (GOYA, n = 552; MAIN, n = 150). Additionally, published gene expression data from 28 DLBCL cell lines<sup>21</sup> and purified, normal ICs<sup>22</sup> were used to assess PD-L1 expression in tumor cells and macrophages, respectively. To quantify the expression of IC subsets, we used immune signatures designed to reflect relevant immune biology (supplemental Table 1) and calculated signature scores by first z score, normalizing expression values of each gene across patients and then calculating an average z score across signature genes for each patient as previously described.<sup>23</sup> High/low expression of each gene signature was determined by median cutoffs. Chromosome 9p24.1 amplification was determined among 443 GOYA samples using the FoundationOne Heme platform (Foundation Medicine Incorporated, Cambridge, MA) as previously described.<sup>24</sup> Next-generation sequencing data are publically available at accession #GSE125966.

**Table 1. Patient characteristics**

	n (%)		P
	GOYA (n = 552)	MAIN (n = 225)	
<b>Age, y</b>			.061
Median	63	62	
Range	18-86	21-79	
Male sex	288 (52.2)	107 (47.6)	.268
<b>Region</b>			<.001*
Western Europe	216 (39.1)	91 (40.4)	
Eastern Europe	122 (22.1)	59 (26.2)	
North America	93 (16.8)	17 (7.6)	
Asia	89 (16.1)	13 (5.8)	
Other	32 (5.8)	45 (18.2)	
<b>IPI</b>			.0057†
Low	107 (19.4)	28 (12.5)	
Low-intermediate	194 (35.1)	102 (45.3)	
High-intermediate	161 (29.2)	71 (31.6)	
High	90 (16.3)	24 (10.7)	
<b>ECOG PS</b>			<.001
0-1	490 (88.8)	164 (73.9)	
2-3	62 (11.2)	58 (26.1)	
<b>Ann Arbor stage</b>		n = 223	.204
I and II	134 (24.3)	64 (28.7)	
III and IV	418 (75.8)	159 (71.3)	
Extranodal involvement	364 (65.9)	100 (44.4)	<.001
<b>COO</b>			.184
GCB	298 (55.4)	70 (47.9)	
ABC	151 (28.1)	52 (35.6)	
Unclassified	89 (16.5)	24 (16.4)	
Median follow-up, mo	29.9	24.2	<.001

COO, cell of origin; ECOG PS, Eastern Cooperative Oncology Group performance status.

\*Regional makeup significantly differed, with more South and Central American samples in MAIN (n = 41) vs GOYA (n = 13).

†International Prognostic Index (IPI) groups differed significantly, with more intermediate samples in MAIN.

### Statistical analysis

Computational analysis of RNAseq data was performed in R (version 3.2.2; R Project for Statistical Computing). We used Cox regression to examine associations between these markers and PFS, adjusting for treatment arm, number of planned chemotherapy cycles, International Prognostic Index, and region (GOYA) or treatment arm (ie, bevacizumab) and International Prognostic Index (MAIN).

## Results

### PD-L1 features in DLBCL

Characteristics of the patients with available tumor tissue from both trials are listed in Table 1. Among 433 DLBCL patients (GOYA, n = 232; MAIN, n = 201) with available PD-L1 IHC results, 95% (by SP263) and 85% (by SP142) of patients expressed the PD-L1 protein on cells morphologically most consistent with macrophage/histiocyte origin, whereas a minority (MAIN, n = 20; 10%; GOYA,

n = 14; 5.6%) showed any PD-L1 staining on tumor cells; in benign lymph node tissues, we saw the typical staining pattern for PD-L1 with positive staining on sinusoidal macrophages and scattered intra- and interfollicular cells of macrophage or DC morphology (Figure 1A-B).

Prevalence and staining intensity of PD-L1 differed according to the antibody and protocol used (Figure 1C). SP263 showed the highest overall staining, with 88% to 91% of patients classified as IHC 2+ (>5% positive). The staining profile for SP142 was comparable in GOYA, where TSA amplification was performed, with 70% classified as IHC 2+. However, in MAIN, the SP142 antibody identified significantly fewer positive cells (35% classified as IHC 2+), suggesting that either SP263 staining or SP142 staining with TSA amplification is recommended for capturing the extent of PD-L1 expression in DLBCL.

At the RNA level, among 702 patients with evaluable RNAseq data, *CD274* (PD-L1) mRNA showed generally consistent correlation with PD-L1 staining by IHC, with slightly higher overall correlations observed for SP263 staining (MAIN,  $r = 0.43$ ; GOYA,  $r = 0.53$ ), compared with SP142 (MAIN,  $r = 0.41$ ; GOYA,  $r = 0.43$ ). *CD274* mRNA was also significantly higher among GOYA patients with a chromosome 9p24.1 amplification (n = 18), as determined by FoundationOne Heme ( $P = 5.03 \times 10^{-10}$ ; supplemental Figure 1), reflecting the confounding of tumor and nontumor sources of PD-L1 when assessing total mRNA levels. *CD274* mRNA was higher among patients with the ABC subtype of DLBCL in both the MAIN ( $P = .01$ ; Figure 1D) and GOYA ( $P = .004$ ) cohorts.

### PD-L1 expression is associated with macrophage and STAT3 gene expression

*CD274* mRNA inversely correlated with a B-cell gene signature (MAIN,  $r = -0.55$ ; Figure 2A; GOYA,  $r = -0.32$ ; supplemental Figure 2), with low/undetectable transcripts in a majority of DLBCL cell lines (n = 28) and resting B-cell samples tested (Figure 2B), consistent with prior reports.<sup>8,13,14,22,25</sup> In contrast, there was significantly higher *CD274* mRNA expression in macrophages and DCs (Figure 2B).

To test the hypothesis that high PD-L1 is primarily expressed on tumor-infiltrating macrophages, we used tumor RNAseq data and previously described techniques to estimate tumor IC infiltrates and correlate PD-L1 expression with a previously described macrophage gene expression signature<sup>23,26</sup> (supplemental Table 1). In both cohorts, macrophage gene expression correlated with PD-L1 protein expression (SP263: MAIN,  $r = 0.36$ ; GOYA,  $r = 0.35$ ; Figure 2C-D) and with *CD274* mRNA expression (MAIN,  $r = 0.61$ ; GOYA,  $r = 0.57$ ; Figure 2E-F). Other signatures of a generally activated tumor microenvironment did not correlate with PD-L1 ( $r = 0.16$  for activated fibroblast gene signature;  $r = 0.28$  for activated lymphoid stroma gene signature;  $r = 0.22$  for activated mesenchymal stroma signature), suggesting that other activated immune subsets do not represent the primary source of PD-L1 expression.

To explore mechanistic signaling pathways tied to PD-L1, we analyzed the association of *CD274* mRNA with pathways implicated in controlling PD-L1 expression. *STAT3* ( $r = 0.48$ ) and a *STAT3* gene signature<sup>27</sup> ( $r = 0.63$ ) correlated with *CD274* gene expression (Figure 2G-H), with a strong correlation

between the *STAT3* gene signature and macrophage gene expression ( $r = 0.85$ ).

### PD-L1, macrophage, and STAT3 correlate with clinical outcomes

Among patients treated in MAIN, high PD-L1 protein expression (SP263; IHC 2+, 3+) correlated with prolonged PFS (hazard ratio [HR], 0.44; 95% confidence interval [CI], 0.24-0.80;  $P < .01$ ; Figure 3A) and OS (HR, 0.33; 95% CI, 0.17-0.65;  $P = .0013$ ; supplemental Figure 6A), which was not statistically significant when using the PD-L1 SP142 reagent without TSA amplification (PFS HR, 0.76; 95% CI, 0.43-1.4;  $P = .36$ ; OS HR, 0.49; 95% CI, 0.23-1.00;  $P = .064$ ) or when assessing *CD274* mRNA expression (PFS HR, 0.84; 95% CI, 0.44-1.6;  $P = .58$ ; OS HR, 0.77; 95% CI, 0.34-1.70;  $P = .53$ ; Figure 3A-B; supplemental Figure 6A). The 21 patients treated in MAIN with PD-L1 expression on TCs did not experience significantly different outcomes (data not shown). Among 552 DLBCL patients treated in GOYA, 91% scored high for PD-L1 by SP263 (2+, 3+), with outcomes indistinguishable from those of the 22 patients with PD-L1 low staining. The association between high PD-L1 (using SP142; IHC 3+) and prolonged PFS/OS among patients in GOYA did not reach statistical significance (PFS HR, 0.63; 95% CI, 0.37-1.1;  $P = .08$ ; OS HR, 1.4; 95% CI, 0.74-2.5;  $P = .32$ ; Figure 3B; supplemental Figure 6B) and was not seen with SP263 (IHC 3+; PFS HR, 0.92; 95% CI, 0.51-1.7;  $P = .78$ ; OS HR, 1.1; 95% CI, 0.55-2.2;  $P = .77$ ; Figure 3B; supplemental Figure 6B). A significantly higher positron emission tomography complete response rate was observed among patients with high *CD274* mRNA ( $P = .02$ ), particularly among patients with ABC DLBCL ( $P = .0001$ ), and was associated with significantly prolonged OS (HR, 0.6; 95% CI, 0.40-0.90;  $P = .014$ ; supplemental Figure 6B) but not PFS (HR, 0.74; 95% CI, 0.53-1.0;  $P = .066$ ; Figure 3B). In GOYA, the effect of PD-L1 (SP142) on PFS was slightly stronger among the GCB DLBCL subset (GCB HR, 0.31; 95% CI, 0.11-0.91;  $P = .03$ ; ABC HR, 0.47; 95% CI, 0.18-1.2;  $P = .12$ ), with no effect among unclassified DLBCL patients (HR, 3.3; 95% CI, 0.67-17;  $P = .14$ ; Figure 3B).

Consistent with the hypothesis that PD-L1 expression may reflect an abundance of activated tumor-infiltrating macrophages relevant to anti-CD20 response, high expression of the macrophage signature correlated with prolonged PFS (HR, 0.63; 95% CI, 0.45-0.87;  $P = .003$ ; Figure 3C) and OS (HR, 0.54; 95% CI, 0.37-0.78;  $P < .01$ ; supplemental Figure 6B) in GOYA, particularly among the ABC subset (PFS HR, 0.38; 95% CI, 0.18-0.8;  $P = .01$ ) and to a lesser extent among the GCB subset (HR, 0.61; 95% CI, 0.37-1;  $P = .051$ ; Figure 3D-E). A similar, but not statistically significant, finding was observed in MAIN by PFS (HR, 0.76; 95% CI, 0.4-1.4;  $P = .39$ ; supplemental Figure 3) and OS (HR, 0.79; 95% CI, 0.35-1.80;  $P = .57$ ; supplemental Figure 6A), possibly attributable to fewer evaluable patients in MAIN compared with GOYA and inconsistent results among patients treated in the bevacizumab arm (PFS HR, 1.5; 95% CI, 0.63-3.5;  $P = .37$ ; supplemental Figure 5). The macrophage effect was consistent among the ABC (HR, 0.6; 95% CI, 0.22-1.6;  $P = .32$ ) and GCB (HR, 0.79; 95% CI, 0.26-2.3;  $P = .66$ ) DLBCL subsets in MAIN (supplemental Figure 4). Moreover, high *STAT3* mRNA similarly correlated with prolonged PFS (HR, 0.67; 95% CI, 0.48-0.93;  $P = .015$ ; Figure 3F) among patients treated in GOYA,



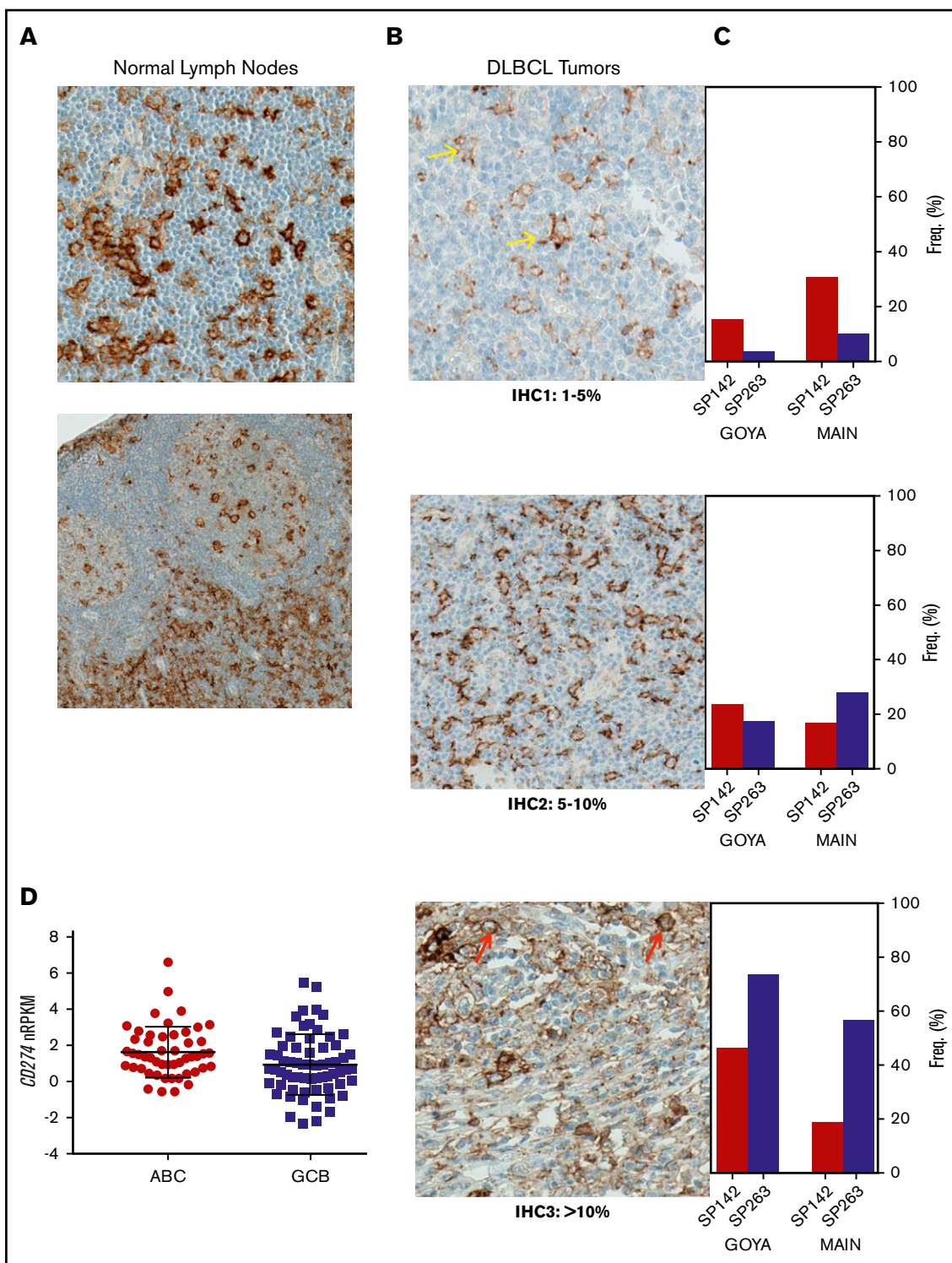
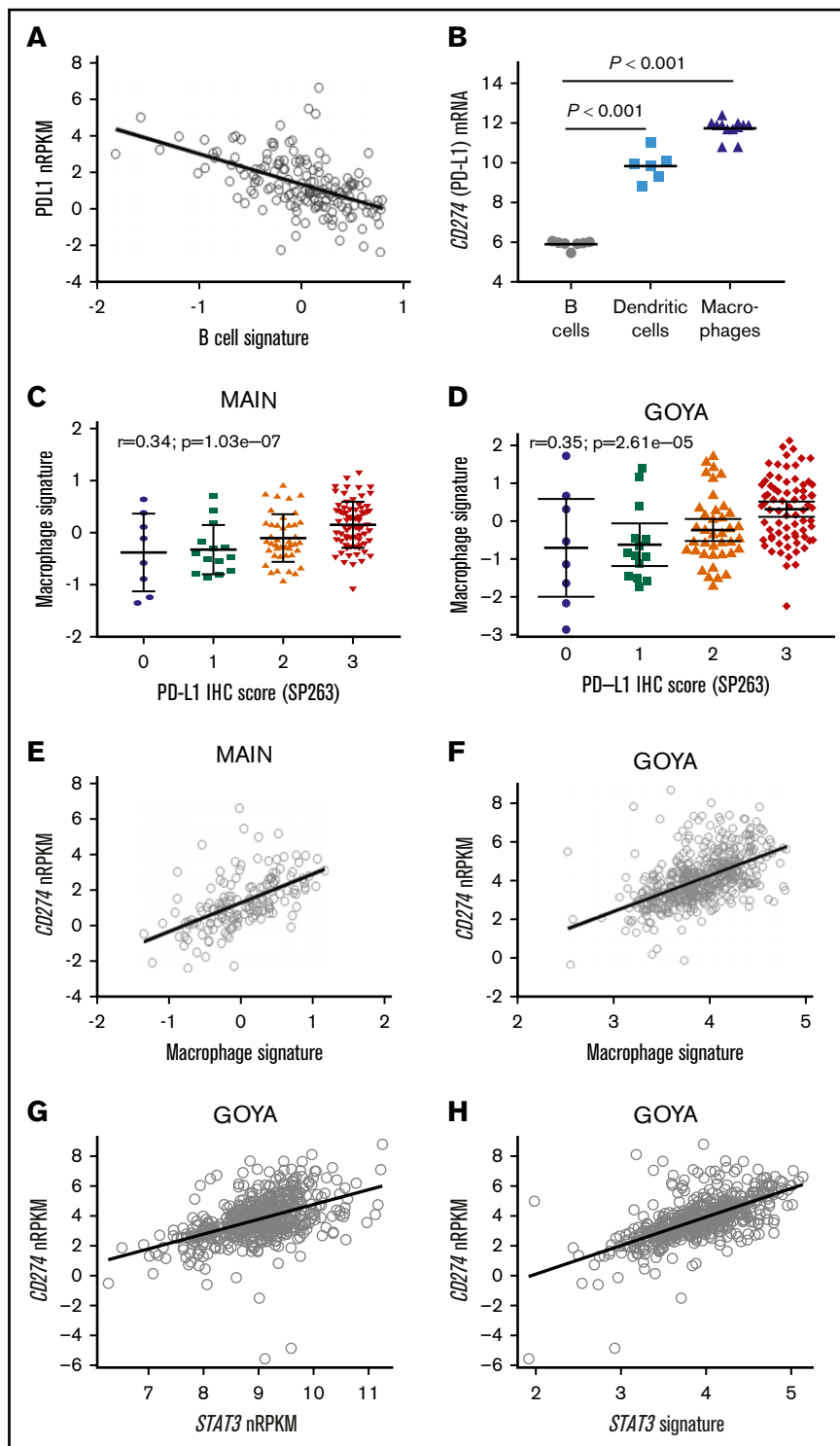


**Figure 1.** Similar to normal lymph nodes, PD-L1 is expressed by myeloid ICs in DLBCL, with different prevalence and intensity depending on the staining procedure. (A) Membranous immunohistochemical stain for PD-L1 protein (with hematoxylin counterstain) on cells with myeloid/dendritic morphology in normal lymph nodes (original magnification  $\times 400$ ). (B) Representative images of PD-L1 protein staining (SP263; original magnification  $\times 400$ ) among DLBCL patients treated in MAIN using a simplified IHC scoring system capturing PD-L1<sup>+</sup> ICs or TCs (IHC 1, 1%-5%; IHC 2, 5%-10%; IHC 3, >10%). Yellow arrows represent PD-L1 staining on myeloid cells, and red arrows represent PD-L1 staining on malignant B cells. (C) PD-L1 prevalence and staining intensity among de novo DLBCL patients treated in 2 phase 3 clinical trials (MAIN, GOYA) using 2 different PD-L1 IHC reagents (SP142, SP263). (D) PD-L1 messenger RNA (mRNA) is higher in the ABC DLBCL subset ( $P = .004$ ; MAIN). Freq, frequency; nRPKM, normalized reads per kilobase million.

**Figure 2. PD-L1 expression correlates with macrophage and STAT3 gene expression.**

(A) *CD274* (PD-L1) mRNA expression inversely correlates with a B-cell gene signature among DLBCL patients treated in MAIN. (B) *CD274* mRNA is highly expressed by purified DCs and macrophages compared with resting B cells. PD-L1 protein expression correlates with a macrophage gene signature among DLBCL patients treated in MAIN (C) and GOYA (D). *CD274* mRNA correlates with a macrophage gene signature among DLBCL patients treated in MAIN (E) and GOYA (F). *CD274* mRNA correlates with *STAT3* gene expression (G) and a *STAT3* gene signature (H) among DLBCL patients treated in GOYA.



suggesting that high *STAT3* signaling among tumor-associated macrophages may contribute to PD-L1 expression in DLBCL.

The macrophage effect was consistent among the ABC (HR, 0.6; 95% CI, 0.22-1.6;  $P = .32$ ) and GCB (HR, 0.79; 95% CI, 0.26-2.3;  $P = .66$ ) DLBCL subsets in MAIN (supplemental Figure 4). Moreover, high *STAT3* mRNA similarly correlated with prolonged

PFS (HR, 0.67; 95% CI, 0.48-0.93;  $P = .015$ ; Figure 3F) among patients treated in GOYA, suggesting that high *STAT3* signaling among tumor-associated macrophages may contribute to PD-L1 expression in DLBCL.

To attempt separation of macrophage subsets, we tested gene signatures designed to estimate the frequency of the M0, M1, and

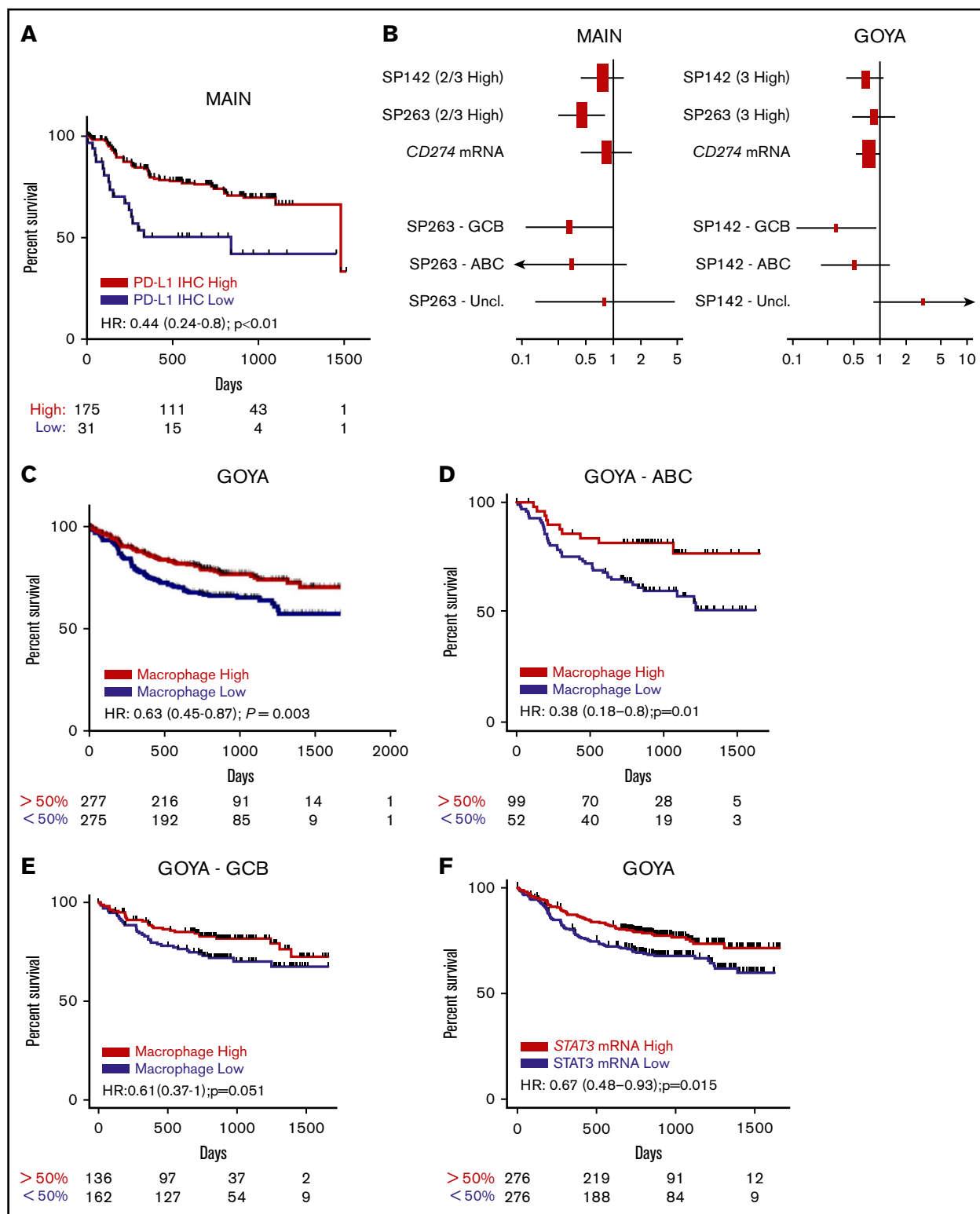


**Figure 3. PD-L1 is not a negative prognostic biomarker in de novo DLBCL and may be associated with better prognosis in some patients, similar to macrophages and STAT3.** (A) High PD-L1 protein expression (IHC 2+, 3+) by SP263 is associated with prolonged PFS in de novo DLBCL (MAIN). (B) Forest plot of HRs and 95% CIs for the association of PD-L1 expression and PFS with regard to different PD-L1 IHC reagents (SP142, SP263), the PD-L1 transcript (*CD274* mRNA), and distinct DLBCL COO subgroups in MAIN and GOYA. High expression of a macrophage gene signature correlates with prolonged PFS (C) and adds prognostic information to DLBCL COO (D-E). (F) High expression of *STAT3* mRNA correlates with prolonged PFS in de novo DLBCL (GOYA). Hazard ratios adjusted for IPI and treatment (MAIN) or IPI, treatment, region, and number of chemotherapy cycles (GOYA). Uncl, unclassified.

M2 macrophage phenotypes<sup>28</sup> (supplemental Table 1). The M1 and M2 signatures were highly correlated with each other ( $r = 0.92$ ) and with the undifferentiated M0 signature ( $r > 0.8$ ), making it difficult to assess the independent contribution of each signature. Only the gene signature designed to estimate the undifferentiated M0 macrophage subset was associated with statistically significant prolonged PFS (HR, 0.65; 95% CI, 0.47-0.91;  $P = .012$ ); neither the M1 nor M2 signature was significantly associated with PFS (M1: HR, 0.8; 95% CI, 0.58-1.1;  $P = .17$ ; M2: HR, 0.84; 95% CI, 0.61-1.2;  $P = .3$ ).

## Discussion

In this current study, we tested the hypothesis that PD-L1 expression reflects abundance of activated tumor-infiltrating macrophages and may not be associated with worse outcomes, in contrast to solid tumors, among de novo DLBCL patients treated with chemoimmunotherapy. Despite very low levels of PD-L1 in normal B cells, reports of PD-L1 expression in B-cell malignancies are conflicting, with different B-cell tumors expressing PD-L1 at varying levels and on different cell populations within the tumor microenvironment. Careful consideration of both TC and IC PD-L1 expression may be important for predicting responses to PD-1/PD-L1 checkpoint blockade, as seen in solid tumors.<sup>29</sup> In classical Hodgkin lymphoma (cHL), PD-L1 is detected on malignant Reed-Sternberg cells in a large majority of patients (70% to 80%) because of alterations in 9p24.1, which harbors the PD-L1 locus. Reed-Sternberg cells, however, comprise only a small proportion of the total tumor bulk (ie, 5% to 10%) in cHL, and a majority of PD-L1-expressing cells in cHL are macrophages.<sup>30</sup> In other B-cell malignancies like follicular lymphoma, marginal zone lymphoma, mantle cell lymphoma, and Burkitt lymphoma, PD-L1 is rarely found on neoplastic B cells (10%, 5%, 0%, and 0%, respectively),<sup>13,31-33</sup> with low levels of PD-L1 expression detectable on intratumoral histiocytes and regulatory T cells. Our data confirm that in DLBCL, PD-L1 expression by malignant B cells is low, with expression primarily restricted to tumor-infiltrating myeloid cells.

We observed surprising biases in PD-L1 staining depending on the IHC assay and protocol used. Overall, SP263 showed the highest staining intensity in both DLBCL cohorts and was the most correlated with *CD274* mRNA expression. The SP142 antibody stained significantly fewer PD-L1<sup>+</sup> cells in MAIN, but with TSA amplification in GOYA, it was roughly comparable to SP263. These results may help explain some of the conflicting results regarding the prognostic effect of PD-L1 in DLBCL,<sup>8,34</sup> which may be important for interpreting clinical data for PD-1/PD-L1 checkpoint blockade in this indication. Moreover, these results highlight the importance of standardizing PD-L1 assay reagents and staining procedures in DLBCL, if PD-L1 becomes a relevant biomarker for anti-PD-1/PD-L1 therapies.

Despite the well-established negative prognostic effect of PD-L1 expression in solid tumors, our data demonstrate that among de novo DLBCL patients treated with chemoimmunotherapy, PD-L1 expression on non-TCs is not a negative prognostic biomarker and in fact may be associated with better prognosis. In this setting, the biologic and prognostic effects of PD-L1 may be due to its role as a proxy for macrophage infiltration and may be particularly dependent upon anti-CD20 monoclonal antibody (mAb) therapy. The PD-L1 correlation with improved outcomes in MAIN using SP263 was

seen to a lesser extent in patients treated in GOYA, but it was only statistically significant among GCB DLBCL patients using the SP142 PD-L1 reagent with TSA amplification. These data from 2 large phase 3 studies suggest that PD-L1 is not a reliable prognostic biomarker in de novo DLBCL, and differences in IHC reagents or patient subsets may affect the clinical significance of PD-L1 expression.

Macrophages are important mediators of antibody-dependent phagocytosis (ADCP), and preclinical studies have demonstrated that macrophages are required for responses to anti-CD20 (rituximab/obinutuzumab) therapy.<sup>35,36</sup> In the absence of anti-CD20 mAb, tumor-associated macrophages may provide a nurturing microenvironment for malignant B cells.<sup>37,38</sup> The treatment dependency of this bidirectional influence of tumor-associated macrophages is supported by other studies of the prognostic impact of myeloid cells on B-cell malignancies.<sup>39</sup> Markers of macrophage infiltration are associated with worse outcomes in both DLBCL and Hodgkin lymphoma patients treated with chemotherapy in the absence of anti-CD20 mAb immunotherapy and with better outcomes when rituximab is added to chemotherapy in de novo DLBCL.<sup>39,40</sup> Our data suggest that PD-L1 correlates with markers of tumor-infiltrating macrophages in DLBCL, possibly reflecting an activated macrophage subset primed for ADCP and contributing to better outcomes among patients treated with modern immunochemotherapy. Interestingly, high expression of the macrophage gene signature added prognostic information to tumor cell of origin and was validated in ABC DLBCL in our MAIN cohort, suggesting a novel tumor-microenvironment interaction and the potential importance of ADCP in the ABC subset.

Macrophages exist in different functional states, the most common of which are the M0 (resting), M1 (classically activated), and M2 (alternatively activated) macrophages. The M2 macrophage phenotype has been linked with highly active phagocytosis of anti-CD20-bound TCs<sup>41</sup>; however, it has been reported that a high concentration of tumor-associated M2 macrophages results in worse DFS in R-CHOP-treated de novo DLBCL patients.<sup>42</sup> We attempted to determine the functional state of the tumor-infiltrating macrophages by using gene signatures that reflect the M0, M1, or M2 phenotype and compared these signatures with our general macrophage signature. All macrophage signatures were highly correlated, making it a challenge to demonstrate that any one subset is more prevalent than the other. Despite the strong correlations, only the M0 macrophage signature demonstrated the same prognostic effect as the general macrophage signature used in this study. Future work will need to explore the function of the different macrophage subsets separately to determine how they contribute to response to anti-CD20 therapy.

Previously published results using multiplex immunofluorescence<sup>43</sup> and unpublished studies have shown that PD-L1 expression can be seen in CD68<sup>+</sup> macrophages and CD11c<sup>+</sup> DCs; this has been observed in benign lymphoid tissues as well as diverse tumor indications. A limitation of our current study is that the determination of PD-L1<sup>+</sup> cells (ie, TCs vs non-TCs) was made based on morphologic/cytologic features (nuclear pleomorphism, prominent nucleoli, high nuclear/cytoplasmic ratio). The limited tissue available from these studies prevented us from performing the ideal dual stains with lineage-specific markers to more specifically define the cells expressing PD-L1. The morphologic features of



the PD-L1<sup>+</sup> cells together with the documented high prevalence of macrophages within DLBCL tissues<sup>44</sup> suggest that many PD-L1<sup>+</sup> cells belong to the macrophage lineage, although there are likely other cell populations that stain for PD-L1. Among tumor biopsies from 3 evaluable DLBCL patients from a separate cohort, we performed quantitative CD68 and PD-L1 colocalization IHC experiments. In all 3 cases, we saw clear PD-L1 and CD68 colocalization, with 1.2% to 18.9% of the tumor area occupied by CD68<sup>+</sup> cells, and 30% to 52% of the CD68<sup>+</sup> cells costained with PD-L1. Future work is planned to more robustly calculate the total number of PD-L1 and CD68 coexpressing cells in a separate cohort and to determine if high coexpression of these 2 markers is similarly associated with outcome.

To further explore mechanistic insights, we performed additional analyses of gene signatures with PD-L1 IHC results, focusing on macrophage subsets and signaling pathways controlling PD-L1 expression. Cytokines such as interferon  $\gamma$  and tumor necrosis factor  $\alpha$ , as well as cytokine signaling pathways such as NF- $\kappa$ B and Stat3, have been shown to regulate PD-L1 expression.<sup>45</sup> Certain lymphomas have also been shown to produce soluble factors like interleukin-10, which may polarize the tumor microenvironment and potentially induce PD-L1 expression on tumor-resident macrophages. In our DLBCL cohorts, high *STAT3* expression correlated with PD-L1 and macrophage gene expression and prolonged PFS among patients treated in GOYA, suggesting a functional relationship between *STAT3* signaling, macrophages, and PD-L1 expression in de novo DLBCL.

The role of PD-L1-expressing myeloid cells in mediating a clinical benefit of anti-PD-1/PD-L1 and anti-CD20 immunotherapies merits additional research. Recent mechanistic studies in mice suggest that DC PD-L1 expression may play an important role in mediating anti-PD-L1 benefit.<sup>46</sup> DC ablation before anti-PD-L1 treatment in tumor-bearing mice compromises anti-PD-L1 efficacy, because

anti-PD-L1 treatment induces DC maturation, leading to T-cell proliferation.<sup>46</sup> Similarly, in tumors containing PD-1-expressing macrophages, treatment with anti-PD-L1 led to increased phagocytosis and tumor clearance.<sup>47</sup> Future studies should explicitly examine the effect of PD-L1-expressing myeloid cell subsets on clinical outcomes and phagocytic potential, with implications for anti-CD20, anti-PD-1/PD-L1, and other myeloid targeting therapies like anti-CSF1R.

## Acknowledgments

The authors acknowledge Guiyuan Lei for statistical support, Kirsten Mundt for MAIN sample collection, and Nancy Valente, Michael Wenger, Ira Mellman, Kartik Krishnan, Ron Mazumder, Wayne Chu, Priti Hegde, and Lukas Amler for thoughtful comments and review.

This work was supported with funding provided by F. Hoffmann-La Roche, Ltd.

## Authorship

Contribution: J.M.V., R.M., and C.R.B. conceived the project, designed and performed the data analysis and interpretation, and prepared the manuscript; H.K. and E.E.K. designed and performed immunohistochemistry experiments and assembled the data; M.Z.O., T.N., and L.H.S. assisted in data collection and interpretation; and all authors approved the final manuscript.

Conflict-of-interest disclosure: C.R.B., R.M., H.K., E.E.K., and J.M.V. are employed by Genentech and are shareholders in F. Hoffman-La Roche. M.Z.O. and T.N. are employed by, and are shareholders in, F. Hoffman-La Roche. L.H.S. declares no competing financial interests.

ORCID profile: E.E.K., 0000-0003-3030-6628.

Correspondence: Jeffrey M. Venstrom, Genentech, Inc., 1 DNA Way, South San Francisco, CA 94080; e-mail: venstroj@gene.com.

## References

1. Curiel TJ, Wei S, Dong H, et al. Blockade of B7-H1 improves myeloid dendritic cell-mediated antitumor immunity. *Nat Med*. 2003;9(5):562-567.
2. Ohigashi Y, Sho M, Yamada Y, et al. Clinical significance of programmed death-1 ligand-1 and programmed death-1 ligand-2 expression in human esophageal cancer. *Clin Cancer Res*. 2005;11(8):2947-2953.
3. Thompson RH, Kuntz SM, Leibovich BC, et al. Tumor B7-H1 is associated with poor prognosis in renal cell carcinoma patients with long-term follow-up. *Cancer Res*. 2006;66(7):3381-3385.
4. Webb JR, Milne K, Kroeger DR, Nelson BH. PD-L1 expression is associated with tumor-infiltrating T cells and favorable prognosis in high-grade serous ovarian cancer. *Gynecol Oncol*. 2016;141(2):293-302.
5. Kim HR, Ha SJ, Hong MH, et al. PD-L1 expression on immune cells, but not on tumor cells, is a favorable prognostic factor for head and neck cancer patients. *Sci Rep*. 2016;6:36956.
6. Lau J, Cheung J, Navarro A, et al. Tumour and host cell PD-L1 is required to mediate suppression of anti-tumour immunity in mice. *Nat Commun*. 2017;8:14572.
7. Tang H, Liang Y, Anders RA, et al. PD-L1 on host cells is essential for PD-L1 blockade-mediated tumor regression. *J Clin Invest*. 2018;128(2):580-588.
8. Kiyasu J, Miyoshi H, Hirata A, et al. Expression of programmed cell death ligand 1 is associated with poor overall survival in patients with diffuse large B-cell lymphoma. *Blood*. 2015;126(19):2193-2201.
9. Rossille D, Gressier M, Damotte D, et al; Groupe Ouest-Est des Leucémies et Autres Maladies du Sang. High level of soluble programmed cell death ligand 1 in blood impacts overall survival in aggressive diffuse large B-Cell lymphoma: results from a French multicenter clinical trial. *Leukemia*. 2014;28(12):2367-2375.
10. Kwicinska A, Tsesmetzis N, Ghaderi M, Kis L, Saft L, Rassidakis GZ. CD274 (PD-L1)/PDCD1 (PD-1) expression in de novo and transformed diffuse large B-cell lymphoma. *Br J Haematol*. 2018;180(5):744-748.



11. Rossille D, Azzaoui I, Feldman AL, et al. Soluble programmed death-ligand 1 as a prognostic biomarker for overall survival in patients with diffuse large B-cell lymphoma: a replication study and combined analysis of 508 patients. *Leukemia*. 2017;31(4):988-991.
12. Hayano A, Komohara Y, Takashima Y, et al. Programmed cell death ligand 1 expression in primary central nervous system lymphomas: a clinicopathological study. *Anticancer Res*. 2017;37(10):5655-5666.
13. Andorsky DJ, Yamada RE, Said J, Pinkus GS, Betting DJ, Timmerman JM. Programmed death ligand 1 is expressed by non-hodgkin lymphomas and inhibits the activity of tumor-associated T cells. *Clin Cancer Res*. 2011;17(13):4232-4244.
14. Chen BJ, Chapuy B, Ouyang J, et al. PD-L1 expression is characteristic of a subset of aggressive B-cell lymphomas and virus-associated malignancies. *Clin Cancer Res*. 2013;19(13):3462-3473.
15. Balar AV, Galsky MD, Rosenberg JE, et al; IMvigor210 Study Group. Atezolizumab as first-line treatment in cisplatin-ineligible patients with locally advanced and metastatic urothelial carcinoma: a single-arm, multicentre, phase 2 trial. *Lancet*. 2017;389(10064):67-76.
16. Fehrenbacher L, Spira A, Ballinger M, et al; POPLAR Study Group. Atezolizumab versus docetaxel for patients with previously treated non-small-cell lung cancer (POPLAR): a multicentre, open-label, phase 2 randomised controlled trial. *Lancet*. 2016;387(10030):1837-1846.
17. Vitolo U, Trněný M, Belada D, et al. Obinutuzumab or rituximab plus cyclophosphamide, doxorubicin, vincristine, and prednisone in previously untreated diffuse large B-cell lymphoma. *J Clin Oncol*. 2017;35(31):3529-3537.
18. Seymour JF, Pfreundschuh M, Trněný M, et al; MAIN Study Investigators. R-CHOP with or without bevacizumab in patients with previously untreated diffuse large B-cell lymphoma: final MAIN study outcomes. *Haematologica*. 2014;99(8):1343-1349.
19. Wright G, Tan B, Rosenwald A, Hurt EH, Wiestner A, Staudt LM. A gene expression-based method to diagnose clinically distinct subgroups of diffuse large B cell lymphoma. *Proc Natl Acad Sci USA*. 2003;100(17):9991-9996.
20. Vennapusa B, Baker B, Kowanetz M, et al. Development of a PD-L1 complementary diagnostic immunohistochemistry assay (SP142) for atezolizumab. *Appl Immunohistochem Mol Morphol*. 2019;27(2):92-100.
21. Dornan D, Bennett F, Chen Y, et al. Therapeutic potential of an anti-CD79b antibody-drug conjugate, anti-CD79b-vc-MMAE, for the treatment of non-Hodgkin lymphoma. *Blood*. 2009;114(13):2721-2729.
22. Abbas AR, Baldwin D, Ma Y, et al. Immune response in silico (IRIS): immune-specific genes identified from a compendium of microarray expression data. *Genes Immun*. 2005;6(4):319-331.
23. Bolen CR, McCord R, Huet S, et al. Mutation load and an effector T-cell gene signature may distinguish immunologically distinct and clinically relevant lymphoma subsets. *Blood Adv*. 2017;1(22):1884-1890.
24. Frampton GM, Fichtenholtz A, Otto GA, et al. Development and validation of a clinical cancer genomic profiling test based on massively parallel DNA sequencing. *Nat Biotechnol*. 2013;31(11):1023-1031.
25. Azzaoui I, Uhel F, Rossille D, et al. T-cell defect in diffuse large B-cell lymphomas involves expansion of myeloid-derived suppressor cells. *Blood*. 2016;128(8):1081-1092.
26. Bindea G, Mlecnik B, Tosolini M, et al. Spatiotemporal dynamics of intratumoral immune cells reveal the immune landscape in human cancer. *Immunity*. 2013;39(4):782-795.
27. Liberzon A, Birger C, Thorvaldsdóttir H, Ghandi M, Mesirov JP, Tamayo P. The Molecular Signatures Database (MSigDB) hallmark gene set collection. *Cell Syst*. 2015;1(6):417-425.
28. Newman AM, Liu CL, Green MR, et al. Robust enumeration of cell subsets from tissue expression profiles. *Nat Methods*. 2015;12(5):453-457.
29. Rittmeyer A, Barlesi F, Waterkamp D, et al; OAK Study Group. Atezolizumab versus docetaxel in patients with previously treated non-small-cell lung cancer (OAK): a phase 3, open-label, multicentre randomised controlled trial. *Lancet*. 2017;389(10066):255-265.
30. Carey CD, Gusenleitner D, Lipschitz M, et al. Topological analysis reveals a PD-L1-associated microenvironmental niche for Reed-Sternberg cells in Hodgkin lymphoma. *Blood*. 2017;130(22):2420-2430.
31. Carreras J, Lopez-Guillermo A, Roncador G, et al. High numbers of tumor-infiltrating programmed cell death 1-positive regulatory lymphocytes are associated with improved overall survival in follicular lymphoma. *J Clin Oncol*. 2009;27(9):1470-1476.
32. Menter T, Bodmer-Haeckl A, Dirnhofer S, Tzankov A. Evaluation of the diagnostic and prognostic value of PDL1 expression in Hodgkin and B-cell lymphomas. *Hum Pathol*. 2016;54:17-24.
33. Xerri L, Chetaille B, Serriari N, et al. Programmed death 1 is a marker of angioimmunoblastic T-cell lymphoma and B-cell small lymphocytic lymphoma/chronic lymphocytic leukemia [published correction appears in *Hum Pathol*. 2010;41(11):1655]. *Hum Pathol*. 2008;39(7):1050-1058.
34. Kwon D, Kim S, Kim PJ, et al. Clinicopathological analysis of programmed cell death 1 and programmed cell death ligand 1 expression in the tumour microenvironments of diffuse large B cell lymphomas. *Histopathology*. 2016;68(7):1079-1089.
35. Gong Q, Ou Q, Ye S, et al. Importance of cellular microenvironment and circulatory dynamics in B cell immunotherapy. *J Immunol*. 2005;174(2):817-826.
36. Uchida J, Hamaguchi Y, Oliver JA, et al. The innate mononuclear phagocyte network depletes B lymphocytes through Fc receptor-dependent mechanisms during anti-CD20 antibody immunotherapy. *J Exp Med*. 2004;199(12):1659-1669.
37. Biswas SK, Mantovani A. Macrophage plasticity and interaction with lymphocyte subsets: cancer as a paradigm. *Nat Immunol*. 2010;11(10):889-896.
38. Zheng Y, Cai Z, Wang S, et al. Macrophages are an abundant component of myeloma microenvironment and protect myeloma cells from chemotherapy drug-induced apoptosis. *Blood*. 2009;114(17):3625-3628.
39. Steidl C, Lee T, Shah SP, et al. Tumor-associated macrophages and survival in classic Hodgkin's lymphoma. *N Engl J Med*. 2010;362(10):875-885.

40. Riihijärvi S, Fiskvik I, Taskinen M, et al. Prognostic influence of macrophages in patients with diffuse large B-cell lymphoma: a correlative study from a Nordic phase II trial. *Haematologica*. 2015;100(2):238-245.
41. Leidi M, Gotti E, Bologna L, et al. M2 macrophages phagocytose rituximab-opsonized leukemic targets more efficiently than m1 cells in vitro. *J Immunol*. 2009;182(7):4415-4422.
42. Marchesi F, Cirillo M, Bianchi A, et al. High density of CD68+/CD163+ tumour-associated macrophages (M2-TAM) at diagnosis is significantly correlated to unfavorable prognostic factors and to poor clinical outcomes in patients with diffuse large B-cell lymphoma. *Hematol Oncol*. 2015;33(2):110-112.
43. Herbst RS, Soria JC, Kowanetz M, et al. Predictive correlates of response to the anti-PD-L1 antibody MPDL3280A in cancer patients. *Nature*. 2014;515(7528):563-567.
44. Kridel R, Steidl C, Gascoyne RD. Tumor-associated macrophages in diffuse large B-cell lymphoma. *Haematologica*. 2015;100(2):143-145.
45. Horlad H, Ma C, Yano H, et al. An IL-27/Stat3 axis induces expression of programmed cell death 1 ligands (PD-L1/2) on infiltrating macrophages in lymphoma. *Cancer Sci*. 2016;107(11):1696-1704.
46. Mayoux M, Fransen MF, Roller A, et al. Dendritic cells dictate the responsiveness of PD-L1 blockade in cancer [abstract]. *Cancer Res*. 2017;77(13 suppl). Abstract 3658.
47. Gordon SR, Maute RL, Dulken BW, et al. PD-1 expression by tumour-associated macrophages inhibits phagocytosis and tumour immunity. *Nature*. 2017;545(7655):495-499.